Bioorganic & Medicinal Chemistry Letters 20 (2010) 180–183

Contents lists available at ScienceDirect

Bioorganic & Medicinal Chemistry Letters

journal homepage: www.elsevier.com/locate/bmcl

Novel lead for potent inhibitors of breast cancer resistance protein (BCRP)

Anne Pick, Henrik Müller, Michael Wiese *

Pharmaceutical Institute, University of Bonn, An der Immenburg 4, 53121 Bonn, Germany

ARTICLE INFO

Article history:
Received 21 September 2009
Revised 2 November 2009
Accepted 3 November 2009
Available online 10 November 2009

Keywords:
ABCG2
Inhibitors
Multidrug resistance
BCRP
Hoechst 33342
Pheophorbide A

ABSTRACT

From our modulator library an interesting inhibitor of breast cancer resistance protein (BCRP) was identified. Due to its high inhibitory potency, this compound may serve as a promising novel lead for the design of new and potent modulators. This adds a new structural class to the few known highly active BCRP inhibitors.

The failure in cancer treatment is often associated with the development of Multidrug Resistance (MDR). One important MDR mechanism is the overexpression of certain ATP-binding cassette (ABC) transporters, especially P-glycoprotein (P-gp), Multidrug resistance-associated protein 1 (MRP1) and the Breast Cancer Resistance Protein (BCRP).[1] These transporters use the energy of ATP hydrolysis to decrease the intracellular accumulation of structurally unrelated substances, thus conferring resistance to a broad spectrum of cytostatic compounds.

BCRP, the most recently discovered ABC-transporter, belongs to the ABCG subfamily.[2] It is composed of one single N-terminal intracellular nucleotide binding domain followed by six transmembrane helices. BCRP is considered to be a half-transporter achieving its functionality by either homo- or heterodimerization.[3] Due to the expression of BCRP in excreting organs and physiological barriers it is supposed to play a physiological role in the protection against xenobiotic compounds.[4,5]

BCRP is capable of transporting large molecules with amphiphilic character which can be positively or negatively charged. Transported substrates are, for example, sulfated hormone metabolites, glucuronidated methotrexate,[6] the anticancer drugs mitoxantrone, topotecan, etoposid and flavopiridol.[5,7] One important strategy to overcome BCRP-mediated resistance is the development of potent inhibitors.

According to a classification scheme proposed by Belkacem et al.[8] BCRP inhibitors can be divided into different classes. (i) Compounds that present specific inhibitors, for instance fumitremorgin C[9] as well as its nontoxic, synthetic analogue Ko143[10] and novobiocin;[11] (ii) so called broad-spectrum modulators which are able to interact with P-gp, BCRP and MRP1 showing different inhibitory potencies. Recently it has been shown that the powerful 3rd generation P-gp modulator XR9576 (tariquidar) is also capable to inhibit BCRP function.[12] Another important subgroup of the broad-spectrum blockers contains naturally occurring flavonoids and derivatives like 6-prenylchrysin or tectochrysin which were identified as potent BCRP modulators.[13] Among the broad-spectrum blockers, tyrosine-kinase inhibitors like imatinib and gefitinib[14] form a second interesting subgroup.

Very recently, potent and selective inhibitors of BCRP derived from the P-gp modulator XR9576 have been reported by Kühnle et al.[15] Minor structural modifications led to a change from P-gp to BCRP inhibition. The increase in activity against BCRP was found to be associated with a shift of the hetarylcarboxamido group from the *ortho* to the *meta* position and the introduction of an ester group on the central aromatic core.

Actually, there are only few highly active inhibitors of BCRP known to date, therefore medicinal chemists have to be encouraged to focus on the development of new and potent BCRP modulators. In this study we present a new promising lead for the design of BCRP modulators with high biological activity.

From our modulator library new compounds which are structurally related to XR9576[16,17] were identified inhibiting BCRP at low micro molar concentrations. These modulators contain a tetrahydroisoquinoline-ethylphenyl substructure which is connected via an amide or urea linker to a hydrophobic part. In our present study, the influence of different linker types was investigated.

* Corresponding author. Tel.: +49 228 735213; fax: +49 228 737929.
E-mail address: mwiese@uni-bonn.de (M. Wiese).

0960-894X/$ - see front matter © 2009 Elsevier Ltd. All rights reserved.
doi:10.1016/j.bmcl.2009.11.004

Regarding their basic structures the compounds can be divided into five subgroups (Fig. 1). Representatives from subgroups 1 and 2 contain only one urea or amide substructure resulting in a molecular weight of only about 400 Da. Subgroups 3, 4 and 5 include compounds with two linkers; either identical or different plus an additional aromatic ring system leading to higher molecular weight (Fig. 1).

The Hoechst 33342 assay[18,19] served as an appropriate test system to determine the inhibitory activity against BCRP in MCF-7 MX cells.[20,21] The substances were additionally analyzed with the BCRP specific substrate pheophorbide A by flow cytometry detection using stably transfected MDCK BCRP cells.[22–24] Table 1 includes the structural features of the studied compounds together with the inhibitory potencies obtained in the Hoechst 33342 and in the pheophorbide A assays which are highly correlated ($r^2 = 0.97$). Further, Table 1 contains the IC_{50}-values of standard compounds like the nontoxic fumitremorgin C analogue Ko143, the aminocoumarin antibiotic novobiocin and the broad spectrum inhibitors XR9576 (tariquidar), GF120918 (elacridar), gefitinib and imatinib. While the IC_{50} values in both cell lines are generally in good agreement, Ko143 proved to be threefold more potent in MDCK BCRP cells than in MCF-7 MX cells. To verify, whether this is due to the different substrates or to the cell lines, Ko143 was measured in MDCK BCRP cells with Hoechst 33342 as substrate, and an IC_{50} value of 98 nM was determined. Therefore the discrepancy seems to be more cell-line dependent.

The inhibitors were also investigated against P-gp using the calcein AM[25] and Hoechst 33342 assays.[21] The XR analogues inhibited P-gp function (for more detailed information see Refs.[17,19,26]). Additionally, our compounds were analyzed for their potential interaction with MRP1 applying the calcein AM assay.[25] Most of the compounds led to no inhibition of MRP1 up to 10 μM. Only substances **4a**, **4b** and **5** behaved as very weak MRP1 modulators with extrapolated IC_{50}-values >20 μM. In agreement with tariquidar, the compounds of the present study should be classified as broad spectrum or dual inhibitors.

With regard to substances based on scaffold 1, derivatives with an *ortho*-nitro substituent (compounds **1a** and **1b**) are clearly more potent than their corresponding amino-analogues (compounds **1d** and **1e**). The activity increases when the nitro group is shifted to the *para*-position (compound **1c**). The reduction of the nitro to an amino group leads to an approximately 20-fold decrease of the inhibitory potency (compound **1f**).

Concerning the representatives of subgroup 2 only minor differences between the biological activities of derivatives carrying an *ortho*-nitro or *ortho*-amino substituent were observed. In accordance with the urea derivatives (scaffold 1) the localization of the nitro-group is essentially directing an interaction with BCRP. Substances **2a** and **2b** are about 10-fold less active than compound **2c**. Again, reduction of the nitro to an amino group in *para*-position leads to a strong decrease of activity (compound **2f**). In Figure 2A the favored conformations of compounds **1b** and **2b** are depicted which were optimized using the MMFF94s force field.[27]

In case of the urea derivative (green) the planar conformation is highly stabilized by a hydrogen bond between the nitro group and the urea nitrogen atom, while for the corresponding amide derivative two conformations, one forming a seven-membered ring hydrogen bond, as shown in Figure 2A, and another with a nitro group pointing 'down' are of nearly equal energy. In both conformations the terminal phenyl ring is tilted by 45° out of the plane. Also, the position of the nitro groups in the conformations shown in Figure 2A differs by 3 Å between **1a/b** and **2a/b**, which also may influence their inhibitory potencies. For the corresponding *ortho*-amino derivatives the picture is reversed. The *ortho*-amino

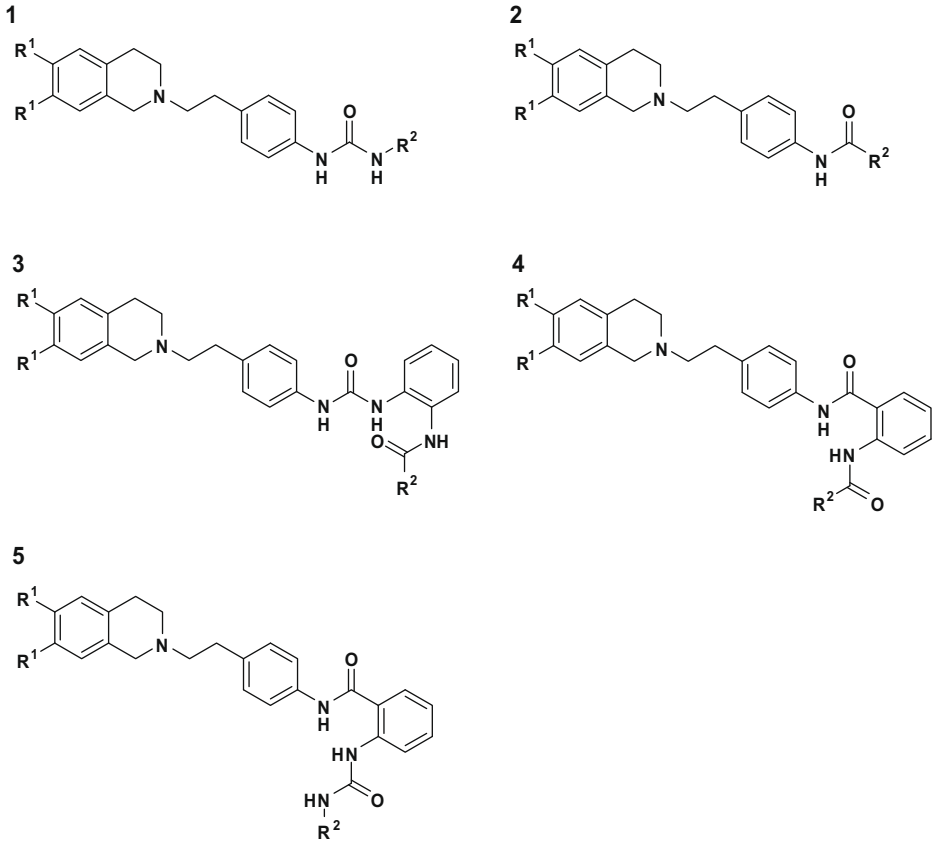

Figure 1. Basic structures of the investigated compounds.

Table 1
Structural features and IC_{50}-values of the investigated compounds

Compds	R^1	R^2	IC_{50} (±SD) μM[a] MCF-7 MX Hoechst assay	IC_{50} (±SD) μM[a] MDCK BCRP pheoA assay
Scaffold 1				
1a	H	2-Nitrophenyl	6.76 (±0.44)	8.71 (±2.37)
1b	OCH_3	2-Nitrophenyl	10.2 (±5.9)	9.08 (±3.29)
1c	OCH_3	4-Nitrophenyl	3.89 (±2.26)	2.61 (±1.41)
1d	H	2-Aminophenyl	102 (±18)	74.1 (±13.9)
1e	OCH_3	2-Aminophenyl	66.1 (±9.4)	58.4 (±13.6)
1f	OCH_3	4-Aminophenyl	74.1 (±12.1)	46.4 (±12.9)
Scaffold 2				
2a	H	2-Nitrophenyl	51.3 (±5.1)	45.7 (±21.9)
2b	OCH_3	2-Nitrophenyl	77.6 (±8.7)	40.0 (±11.1)
2c	OCH_3	4-Nitrophenyl	6.92 (±1.62)	4.38 (±1.70)
2d	H	2-Aminophenyl	17.8 (±1.45)	20.9 (±10.4)
2e	OCH_3	2-Aminophenyl	32.4 (±1.3)	20.7 (±11.1)
2f	OCH_3	4-Aminophenyl	219 (±45)	98.2 (±11.2)
Scaffold 3				
3	OCH_3	3,4-Dimethoxyphenyl	10.2 (±6.1)	6.98 (±3.11)
Scaffold 4				
4a	OCH_3	3,4-Dimethoxyphenyl	0.93 (±0.28)	0.86 (±0.13)
4b	H	4-nitrophenyl	0.69 (±0.34)	0.63 (±0.29)
Scaffold 5				
5	OCH_3	4-Nitrophenyl	0.54 (±0.02)	0.50 (±0.08)
Ko143			0.23 (±0.06)	0.074 (±0.016)
Novobiocin			85.1 (±15.8)	104 (±12)
XR9576			0.68 (±0.05)	0.85 (±0.07)
GF120918			0.40 (±0.03)	0.43 (±0.03)
Gefitinib			1.10 (±0.44)	1.26 (±0.23)
Imatinib			4.07 (±1.34)	3.38 (±1.90)

[a] Values are means of three independent experiments, standard deviations are given in parentheses. Hoechst = Hoechst 33342; pheoA = pheophorbide A assay.

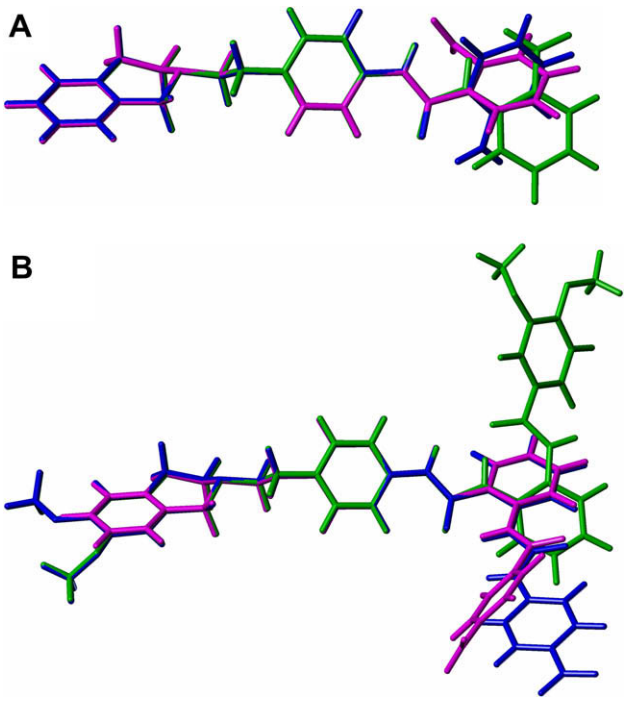

Figure 2. (A) Superposition of the favored conformations of the compounds **1a** (green), **2a** (magenta) and **2d** (blue) pointing out that substance **1a** adopts a more planar conformation with regard to R^2 than its corresponding analogue **2a** or the amino-derivative **2d**. (B) Superposition of representatives with scaffolds 3–5. The urea linker of compound **3** (green) induces an orientation of R^2 which is clearly deviating from that of compounds **4b** (magenta) and **5** (blue).

amide derivative **2d** can adopt a more planar conformation stabilized by a hydrogen bond, although a conformation with opposite orientation of the substituent has the same energy. This observation supports our assumption, that a more planar arrangement of the two phenyl rings is favorable for BCRP inhibition.

The presence of methoxy groups in position 6 and 7 of the tetrahydroisoquinoline substructure seems to possess only a minor influence on activity.

Compound **3** contains an additional aromatic substituent, whose introduction intensifies the interaction with BCRP moderately, in comparison with the amino-analogue based on scaffold 1 (compound **1e**).

However, when the urea linker of compound **3** is replaced by an amide group as in compound **4a** the IC_{50}-value decreases remarkably. Altering the 3,4-dimethoxy- into an electron withdrawing *para*-nitro substituent the activity remains unchanged (compound **4b**).

Among the investigated substances compound **5** was identified as the most potent modulator with an IC_{50} value of about 500 nM in both assays. In comparison with the derivatives based on scaffold 3 the linkers are mutually exchanged.

In Figure 2B the energetically optimized structures of representatives with scaffolds 3–5 are given. The presence of the urea substructure as in compound **3** (green) leads to two preferred conformations within this part. The lowest energy is obtained for a hydrogen bond between urea NH and the carbonyl oxygen of the adjacent amide group, while the opposite hydrogen bonding from carbonyl oxygen of the urea to the amide NH is disfavored by 2 kcal/mol. In both conformations R^2 shows an orientation which strongly deviates from those of the substances **4b** (magenta) and **5** (blue), apparently having a negative influence on activity.

In Figure 3 a typical concentration–response curve of substance **5** is illustrated together with the most potent BCRP inhibitor Ko143, the less active, specific modulator novobiocin and the broad spectrum modulator XR9576 (tariquidar). Due to the high biological activity of compound **5** this modulator can be regarded as promising lead for the design of new and highly active BCRP inhibitors in future.

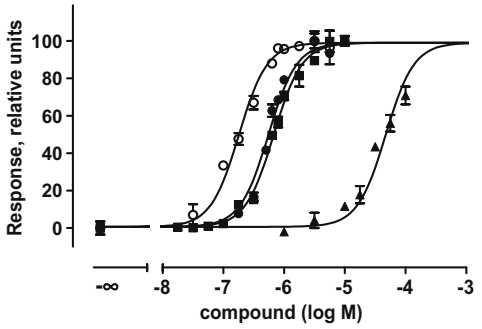

Figure 3. Comparison of the inhibitory potencies of Ko143, XR9576 (tariquidar), novobiocin and compound **5** carried out with the Hoechst 33342 assay in MCF-7 MX cells. pIC_{50} (Ko143) = 6.65 ± 0.03 (open circles), pIC_{50} (compound **5**) = 6.26 ± 0.02 (closed circles), pIC_{50} (XR9576) = 6.17 ± 0.02 (closed squares), pIC_{50} (novobiocin) = 4.21 ± 0.04 (closed triangles). Data shown represents one typical experiment out of a series of three independent experiments.

Acknowledgements

The authors thank Dr. A. H. Schinkel (The Netherlands Cancer Institute, Amsterdam, The Netherlands) for kindly providing Ko143 and the MDCK BCRP cell line.[22] The breast cancer resistant cell line MCF-7 MX[20] was kindly provided by Dr. E. Schneider, Wadsworth Center, Albany, NY, USA. The authors thank further Dr. Armin Buschauer, Institute of Pharmaceutical Chemistry, University of Regensburg, Germany for tariquidar. The work was supported by DFG (Deutsche Forschungsgemeinschaft) grant GRK677.

References and notes

1. Bodo, A.; Bakos, E.; Szeri, F.; Varadi, A.; Sarkadi, B. *Toxicol. Lett.* **2003**, *140–141*, 133.
2. Doyle, L. A.; Yang, W.; Abruzzo, L. V.; Krogmann, T.; Gao, Y.; Rishi, A. K.; Ross, D. D. *Proc. Natl. Acad. Sci. U.S.A.* **1998**, *95*, 15665.
3. Henriksen, U.; Gether, U.; Litman, T. *J. Cell Sci.* **2005**, *118*, 1417.
4. Borst, P.; Evers, R.; Kool, M.; Wijnholds, J. *J. Natl. Cancer Inst.* **2000**, *92*, 1295.
5. Doyle, L. A.; Ross, D. D. *Oncogene* **2003**, *22*, 7340.
6. Suzuki, M.; Suzuki, H.; Sugimoto, Y.; Sugiyama, Y. *J. Biol. Chem.* **2003**, *278*, 22644.
7. Robey, R. W.; Medina-Perez, W. Y.; Nishiyama, K.; Lahusen, T.; Miyake, K.; Litman, T.; Senderowicz, A. M.; Ross, D. D.; Bates, S. E. *Clin. Cancer Res.* **2001**, *7*, 145.
8. Ahmed-Belkacem, A.; Pozza, A.; Macalou, S.; Perez-Victoria, J. M.; Boumendjel, A.; Di Pietro, A. *Anticancer Drugs* **2006**, *17*, 239.
9. Rabindran, S. K.; Ross, D. D.; Doyle, L. A.; Yang, W.; Greenberger, L. M. *Cancer Res.* **2000**, *60*, 47.
10. Allen, J. D.; van Loevezijn, A.; Lakhai, J. M.; van der Valk, M.; van Tellingen, O.; Reid, G.; Schellens, J. H.; Koomen, G. J.; Schinkel, A. H. *Mol. Cancer Ther.* **2002**, *1*, 417.
11. Shiozawa, K.; Oka, M.; Soda, H.; Yoshikawa, M.; Ikegami, Y.; Tsurutani, J.; Nakatomi, K.; Nakamura, Y.; Doi, S.; Kitazaki, T.; Mizuta, Y.; Murase, K.; Yoshida, H.; Ross, D. D.; Kohno, S. *Int. J. Cancer* **2004**, *108*, 146.
12. Clark, R.; Kerr, I. D.; Callaghan, R. *Br. J. Pharmacol.* **2006**, *149*, 506.
13. Ahmed-Belkacem, A.; Pozza, A.; Munoz-Martinez, F.; Bates, S. E.; Castanys, S.; Gamarro, F.; Di Pietro, A.; Perez-Victoria, J. M. *Cancer Res.* **2005**, *65*, 4852.
14. Yanase, K.; Tsukahara, S.; Asada, S.; Ishikawa, E.; Imai, Y.; Sugimoto, Y. *Mol. Cancer Ther.* **2004**, *3*, 1119.
15. Kühnle, M.; Egger, M.; Müller, C.; Mahringer, A.; Bernhardt, G.; Fricker, G.; König, B.; Buschauer, A. *J. Med. Chem.* **2009**, *52*, 1190.
16. Roe, M.; Folkes, A.; Ashworth, P.; Brumwell, J.; Chima, L.; Hunjan, S.; Pretswell, I.; Dangerfield, W.; Ryder, H.; Charlton, P. *Bioorg. Med. Chem. Lett.* **1999**, *9*, 595.
17. Klinkhammer, W.; Müller, H.; Globisch, C.; Pajeva, I. K.; Wiese, M. *Bioorg. Med. Chem.* **2009**, *176*, 2524.
18. Müller, H.; Klinkhammer, W.; Globisch, C.; Kassack, M. U.; Pajeva, I. K.; Wiese, M. *Bioorg. Med. Chem.* **2007**, *15*, 7470.
19. Pick, A.; Müller, H.; Wiese, M. *Bioorg. Med. Chem.* **2008**, *16*, 8224.
20. MCF-7 MX cells were cultured in RPMI 1640 medium supplemented with 10% fetal bovine serum, 50 μl/ml streptomycin and 50 U/ml penicillin G (1% in cell culture medium). Cells were maintained at 37 °C in a humidified atmosphere containing 5% CO_2. When achieving a confluence of 80–90% cells were treated with trypsin–EDTA before subculturing. Every 5th passage mitoxantrone (0.1 μM final concentration) was added to the cell culture medium to maintain ABCG2 overexpression. Before performing an experiment, mitoxantrone was removed from the cell suspension and cells were cultivated at least one passage in the absence of the cytostatic drug.
21. Determination of the inhibitory potencies: For the investigation of MCF-7 MX cells the Hoechst 33342 assay was used. After a confluence of 80–90% was reached cells were harvested by gentle trypsination and centrifuged. (1200 rpm, 4 °C, 4 min). Subsequently, the cell pellet was resuspended in fresh culture medium and the cell density was determined using a Casy I Model TT cell counter device (Schaerfe System GmbH, Reutlingen, Germany). Followed by another centrifugation cells were washed three times with Krebs-Hepes buffer and seeded into black 96 well plates (Greiner, Frickenhausen, Germany) at a density of approximately 20,000 cells per well in a volume of 90 μl. Into each well, 10 μl of various test compounds in different concentrations were added to a total volume of 100 μl. The prepared 96 well plate was kept under 5% CO_2 and 37 °C for 30 min. After this preincubation period, 20 μl of a 30 μM Hoechst 33342 solution (protected from light) was added to each well. Fluorescence was measured immediately in constant intervals (120 s) up to 4500 s at an excitation wavelength of 355 nm and an emission wavelength of 460 nm applying a 37 °C tempered BMG POLARstar microplate reader. The upper plateau value (Y_{max}-value) of each fluorescence-time curve was determined based on one-phase exponential curve fitting. The obtained Y_{max}-values were defined as responses. From these data, concentration-response curves were generated by nonlinear regression using the 4-parameter logistic equation with variable Hill slope (GRAPHPAD PRISM 5.0 software, San Diego, CA).
22. Merino, G.; Jonker, J. W.; Wagenaar, E.; van Herwaarden, A. E.; Schinkel, A. H. *Mol. Pharmacol.* **2005**, *67*, 1758.
23. For the functional investigation of MDCK BCRP cells the pheophorbide A assay was applied. Cells were harvested as described above. After adding different concentrations of the modulators, the fluorescence was measured after a 120 min incubation period with pheophorbide A (final concentration 0.5 μM) applying flow cytometry detection (FACS Calibur, Becton Dickinson, Heidelberg, Germany). Pheophorbide A was excited at a wavelength of 488 nm, and emission was detected in the FL_3 channel (633 nm). Cell debris or dead cells were eliminated by gating on forward versus side scatter. The measured fluorescence was defined as response to generate concentration-response curves corresponding to the procedure described above.
24. We confirmed the overexpression of BCRP in MCF-7 MX and MDCK BCRP cells applying the BCRP specific antibody 5D3 which recognizes an external epitope of BCRP. Following the manufactures preparation procedure equal quantities of MCF-7 MX, MCF-7, MDCK and MDCK BCRP cells were analyzed by flow cytometry detection. The results, presented as geometric means of fluorescence, prove that BCRP is highly overexpressed in MCF-7 MX (215 ± 3) and MDCK BCRP cells (215 ± 3). The labeling of MCF-7 (9.7 ± 0.4) and MDCK cells (9.8 ± 0.3) was negligible illustrating that BCRP is not present in these cells.
25. The cells were prepared as described above and seeded into colorless 96-well plates (Greiner, Frickenhausen, Germany) at a density of approximately 30,000 cells per well (one well including 90 μl cell suspension and 10 μl test compound solution). After the preincubation period with the test compounds, 33 μl of a 1.25 μM calcein AM solution which was protected from light was added to each well. The fluorescence was detected immediately at constant time intervals (120 s) up to 46 min at an excitation wavelength of 485 nm and an emission wavelength of 520 nm applying a 37 °C tempered BMG POLARstar microplate reader. The fluorescence-data points were measured up to 46 min and the slopes were calculated by linear regression and used as dependent parameters. From these data concentration–response curves were generated by nonlinear regression using the 4-parameter logistic equation with variable Hill slope (GRAPHPAD PRISM 5.0 software, San Diego, CA).
26. Müller, H.; Pajeva, I. K.; Globisch, C.; Wiese, M. *Bioorg. Med. Chem.* **2008**, *16*, 2456.
27. As no X-ray data of the compounds were available, the energy minimized conformers were generated using stochastic search. In the stochastic search the MMFF94s force field was applied with the default SYBYL settings. To ensure a better sampling of conformational space the following parameters were defined: energy cut off 10 kcal/mol, failure limit 200 (continuous number of attempts to generate a new conformation), RMS tolerance 0.5, iteration limit 20,000, and minimization iteration limit 2000.